Research Article Open Access

Renbo Wei*#, Qian Xiao#, Chenhao Zhan, Yong You, Xuefei Zhou and Xiaobo Liu*

Polyarylene ether nitrile and boron nitride composites: coating with sulfonated polyarylene ether nitrile

https://doi.org/10.1515/epoly-2019-0009
Received July 17, 2018; accepted August 22, 2018.

Abstract: Boron nitride (BN) coated with sulfonated polyarylene ether nitrile (SPEN) (BN@SPEN) was used as additive to enhance the thermal conductivity of polyarylene ether nitrile. BN@SPEN was prepared by coating BN micro-platelets with SPEN through ultrasonic technology combined with the post-treatment bonding process. The prepared BN@SPEN was characterized by FTIR, TGA, SEM and TEM, which confirmed the successful coating of BN micro-platelets. The obtained BN@SPEN was introduced into the PEN matrix to prepare composite films by a solution casting method. The compatibility between BN and PEN matrix was studied by using SEM observation and rheology measurement. Furthermore, thermal conductivity of BN@SPEN/PEN films were carefully characterized. Thermal conductivity of BN@SPEN/PEN films was increased to 0.69 W/(m · K) at 20 wt% content of BN@SPEN, having 138% increment comparing with pure PEN.

Keywords: polyarylene ether nitrile; boron nitride; surface coating; sulfonated polyarylene ether nitrile

1 Introduction

Polyarylene ether nitrile represents a new polymeric material (1-3). In recent years, both the scientific community and the related commercial groups have aroused great interest in research of PEN, because of its remarkable performances, including prominent thermal and mechanical properties (2-4). The nitrile group bonding on the aromatic ring of PEN exhibits strong polarity which facilitates the adhesion between main-chain of macromolecule and other substances, and visibly increase the dielectric property. Moreover, the second generation of PEN terminated with phthalonitrile has a higher processing temperature and wide range of applications. The introduced phthalonitrile on the terminal point of polyarylene ether nitrile macromolecule main-chain can crosslink to build phthalocyanine rings with high thermal stability (5-7).

To fulfill the application in high temperature atmosphere, it not only requires the material with high temperature resistance, but also with excellent thermal conductivity (8). Although PEN can feed many demands including high temperature fields and outstanding mechanical domains owing to its unique structure and intrinsic high glass transition temperature (9,10), PEN is considered as a thermal insulator like other polymers with low thermal conductivity (11). The most promising and effective method of improvement of the thermal conductivity of PEN is the incorporation of additives with high thermal conductivity (11). A multitude of additives, such as carbon, metal oxides, metal nitrides, clay (12-14), and boron nitride (BN) (15-18) have been used as the additives to enhance the thermal conductivity of polymers.

Among those high thermally conductive fillers, boron nitride (BN) is mostly studied because of its high temperature stability, superior mechanical strength, a large thermal conductivity and insulating property, etc (19-23). BN is attractive not only in academic research but also with numerous applications because of structural analog and isoelectronic counterpart of graphite (24). In addition, BN has special structure that the strong covalent bonds of BN between boron and nitrogen atoms are formed alternately and BN is a fine electrical insulating two-dimensional material, which leads BN to be a good candidate for the preparation of thermal and

*** Corresponding author: Renbo Wei and Xiaobo Liu,** Research Branch of Advanced Functional Materials, School of Materials and Energy, University of Electronic Science and Technology of China, Chengdu 610054, China, e-mail: weirb10@uestc.edu.cn (Renbo Wei); liuxb@uestc.edu.cn (Xiaobo Liu). Tel. /fax: +86-28-83207326.
Qian Xiao, Chenhao Zhan, Yong You and Xuefei Zhou, Research Branch of Advanced Functional Materials, School of Materials and Energy, University of Electronic Science and Technology of China, Chengdu 610054, China.
#Renbo Wei and Qian Xiao contributed equally to this work.

electrical insulating composites (25-27). Nevertheless, there is still a challenge that BN and polymer matrix show good compatibility.

In this study, the BN was firstly coated with sulfonated polyarylene ether nitrile (SPEN) offering BN@SPEN, and then the BN@SPEN was introduced into polyarylene ether nitrile (PEN) matrix to obtain BN@SPEN/PEN composites. FTIR, TGA, SEM and TEM confirmed the preparation of BN@SPEN. The SEM and rheometer were used to study the compatibility between BN and PEN. Improved thermal conductivity of PEN was observed after the incorporation of the BN@SPEN. In addition, thermal, mechanical properties were also carefully investigated.

2 Experimental section

2.1 Materials

BN micro-platelets was received from J&K chemicals. *N*-methylpyrrolidone, toluene and acetone were obtained from KeLong chemicals. 4-Nitrophthalonitrile was purchased from Alpha chemicals. Sigma-Aldrich provided potassium 2,5-dihydroxybenzenesulfonate (PDBS) and 2,6-difluorobenzonitrile (DFBN). HCl and Phenolphthalin (PPL) were obtained from Haihong Chemicals. Potassium carbonate (K_2CO_3), hydroquinone (HQ) and biphenyl (BP) were used as received without other treatment.

2.2 Synthesis of PEN and SPEN

Synthesis of PEN terminated with phthalonitrile (Figure 1) by nucleophilic aromatic substitution polymerization method was accorded to the previous literature (28). Sulfonated polyarylene ether nitrile (SPEN, Figure 1) used in this work was synthesized according to the literature via nucleophilic aromatic substitution reaction between PPL, PDBS and DFBN (29).

2.3 Preparation of BN@SPEN

The BN@SPEN was obtained by ultrasonic method combined with the post-treatment bonding process. BN micro-platelets (1.0 g) was dispersed with 20 mL deionized water in a three neck round bottle flask. A highly dispersed white suspension was obtained with the help of violent ultrasonic treatment and mechanical stirrer for 2 h. Simultaneously, a certain mass (0.4 g) of SPEN was dissolved in 10 mL deionized water with mechanical stirring. Then, the SPEN solution was tenderly transferred into the BN suspension, and then stirred for another 3 h with ultra-sonication. After that, the mixture was further stirred with ultra-sonication at 70°C to evaporate the solvent mostly. The obtained particles were added into a mortar and were grinded into powder. Finally, the sulfonated polyarylene ether nitrile coated BN (BN@SPEN) were obtained after treating at 200°C for 4 h.

2.4 Preparation of BN@SPEN/PEN composites

The BN@SPEN/PEN composite film was fabricated by solution casting method. At first, BN@SPEN with weight mass was added in a three neck flask with 10 mL NMP solvent, forming a dispersion after simultaneously mechanical stirring and ultra-sonication for 2 h. Meanwhile, a certain mass of PEN was transferred into another 100 mL three neck flask and dissolved in NMP solvent. Then, the PEN solution stirring at 100°C for 30 min was mixed with the BN@SPEN dispersion. After cooling down to room temperature, the mixture was further stirred with ultra-sonication for 60 min. At last, above mentioned mixture putting on a glass plate was dried at the temperature of 90, 120, 140 and 160°C each for 1 h and 200°C for 2 h. When the temperature reached the room temperature, BN@SPEN/PEN films with different BN@SPEN loading were obtained. The BN@SPEN/PEN

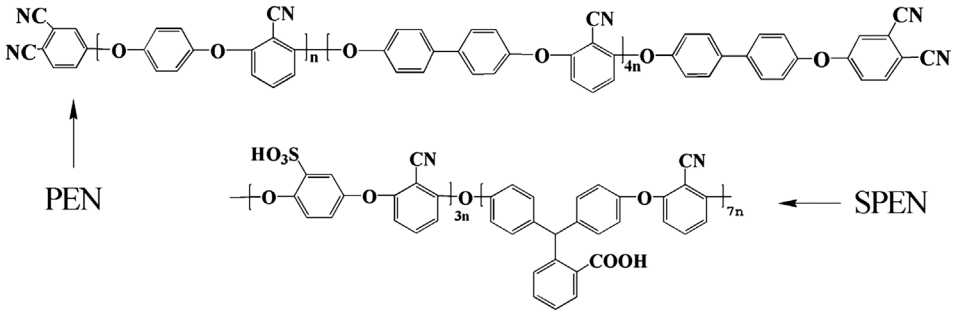

Figure 1: Structure of PEN and SPEN.

films were named as PEN, BN@SPEN/PEN4, BN@SPEN/PEN8, BN@SPEN/PEN12, BN@SPEN/PEN16 and BN@SPEN/PEN20 with BN@SPEN loading of 0, 4, 8, 12, 16 and 20 wt% respectively. Besides, BN/PEN composite film with 8 wt% BN was also prepared for comparison.

2.5 Characterization

FTIR (200SXV, Nicolet) was employed to characterize chemical structure of samples. The pressed specimen mixed with KBr was tested. Morphologies of BN@SPEN and BN@SPEN were characterized by SEM (JEOL, JSM-5900LV) handling at 20 kV. DSC (Q100, TA) was measured from 100 to 320°C at a heat rate of 10°C/min. TGA (Q50, TA) was conducted from 100 to 800°C in nitrogen at a heat rate of 20°C/min. The mechanical measurements were taken on Electromechanical Universal Testing Machine (SANS CMT6104) under ISO-527-3 standard. Dynamic thermomechanical analysis (DMA, Q800, TA) was tested from 50 to 360°C at a heat rate of 5°C/min. Rheometer (AR-G2, TA) with parallel plates was employed for the rheological measurements. Samples (Φ25 mm × 1 mm) were tested at 320°C from 0.10 to 100 rad/s.

3 Result and discussion

3.1 Preparation of BN@SPEN

FTIR was used to verify the coating of BN with SPEN. Figure 2a is FTIR spectra of BN and BN@SPEN. FTIR peak at 1387 cm^{-1} of comes from B-N stretching vibration, FTIR peak at 809 cm^{-1} is B-N-B (30-34), and FTIR peak at 3423 cm^{-1} is ascribed as O-H at the surface of BN. In comparison, the peak at 1016 cm^{-1} on the FTIR spectrum of BN@SPEN is consistent with C-O bond (35), the FTIR band at 1605 cm^{-1} is from benzene rings at SPEN (36), and a weak peak located at 2233 cm^{-1} is consistent with nitrile groups (-CN) on SPEN (37). Figure 2b shows the TGA curves of BN, BN@SPEN and SPEN. TGA results were measured from room temperature to 800°C, and the residual mass at 790°C on the TGA curves were used for the calculation of the BN content in BN@SPEN. The residual mass of BN, SPEN and BN@SPEN at 790°C is 100%, 51.6% and 86.7% respectively. Consequently, the BN content in BN@SPEN is calculated to be 72.6 wt%. SEM was also used to characterize the coating of BN micro-platelets with SPEN (Figures 3a and 3b). The SEM images show that the BN micro-platelets are coated by SPEN shell forming the BN@SPEN. TEM image of BN@SPEN indicates that BN is adhered together by SPEN (Figure 3c). All the evidence is sufficient to prove that the preparation of BN@SPEN is successful.

3.2 Morphology of BN@SPEN/PEN

The structure of PEN is shown in Figure 1. The BN was coated with SPEN (BN@SPEN) to improve the compatibility between BN and PEN. To explore the dispersability and compatibility of BN fillers with the PEN matrix, the micro-morphologies of BN@SPEN/PEN and BN/PEN were investigated by SEM observation under the same weight percent of BN (8.0 wt%). As shown in Figures 4a and 4b, the BN is well dispersed in the PEN matrix in BN@SPEN/PEN due to the SPEN shell on BN@SPEN. In addition, a ductile section with ridge pattern is observed of the cross-section of BN@SPEN/PEN. When 20 wt% of BN@SPEN was incorporated, the BN is still well dispersed in the matrix

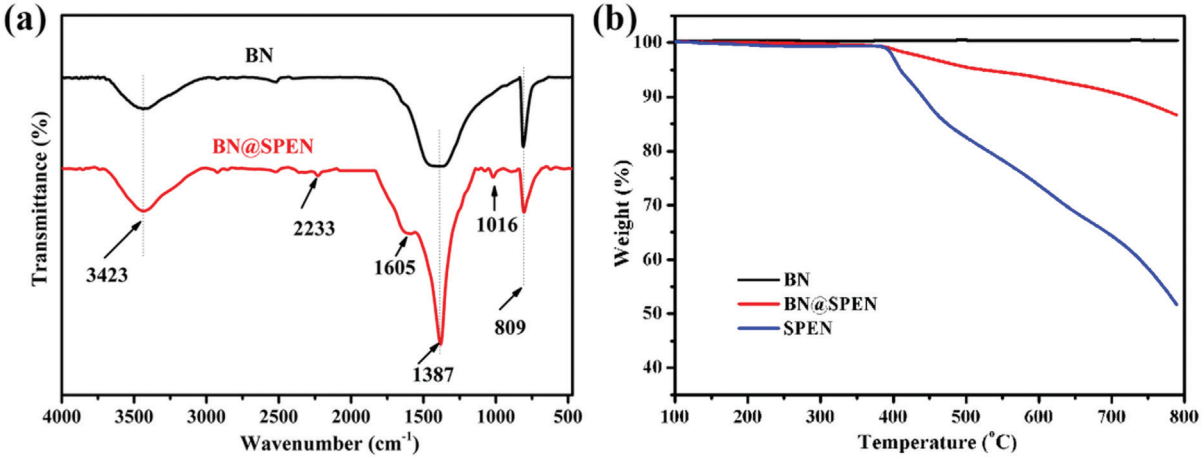

Figure 2: (a) FTIR spectra of the BN@SPEN and BN; (b) TGA curves of BN, BN@SPEN and SPEN.

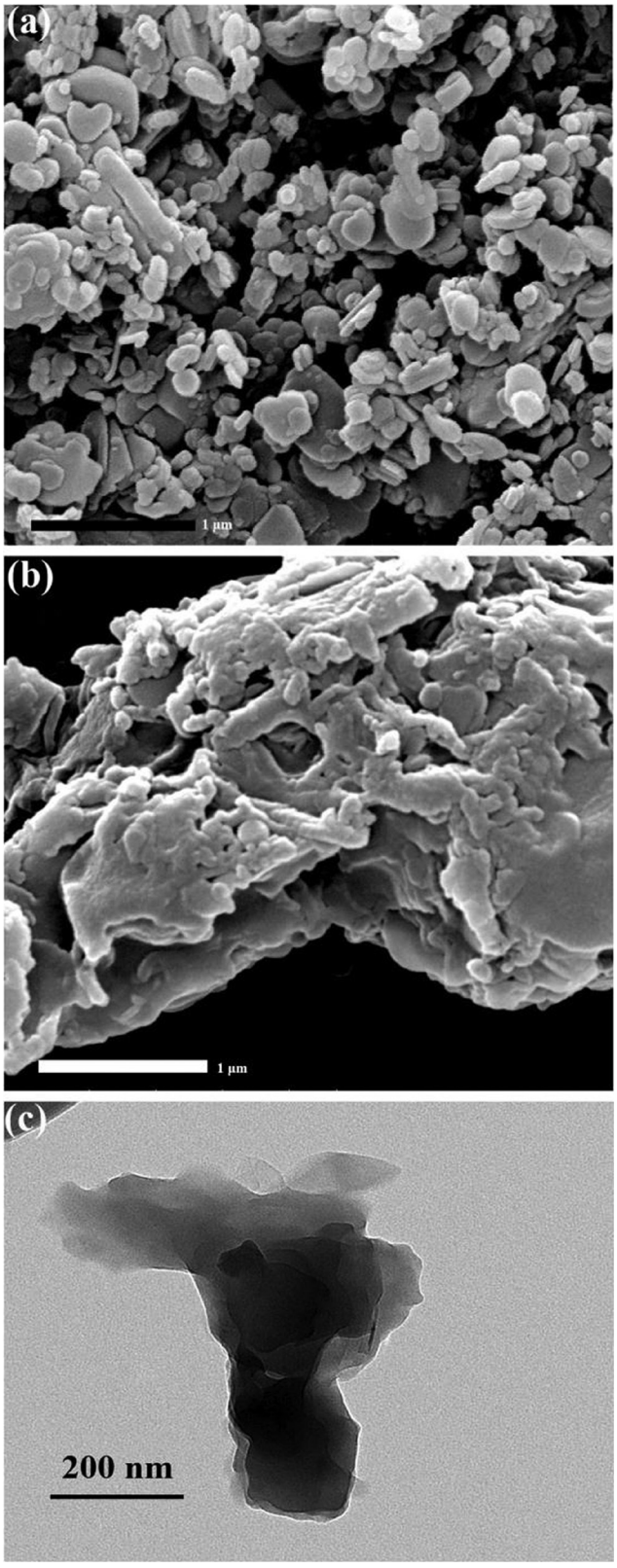

Figure 3: SEM images of (a) BN and (b) BN@SPEN; (c) TEM image of BN@SPEN.

(Figures 4a and 4d). For BN/PEN, the SEM micrographs show that the BN is randomly dispersed on the surface of PEN matrix, indicating the poor compatibility between BN and PEN (Figures 4e and 4f). Meanwhile, the smooth surface of BN on the cross-section of BN/PEN suggests that the BN/PEN film is broken down on the interface of BN and PEN. The different dispersability and compatibility between BN and PEN in BN/PEN and BN@SPEN/PEN should be attributed to those factors: (1) the BN aggregates in PEN matrix due to the different polarities and surface energies between the organic and inorganic phases (32); (2) the SPEN shell hinders the aggregation of BN; (3) the compatibility between the BN@SPEN and PEN matrix is much better than that between BN and PEN.

3.3 Rheological properties of BN@SPEN/PEN

Oscillatory shear rheological measurements were tested at 320°C to explore the relationship between BN and PEN. Figure 5 exhibits complex viscosity (η^*) and storage modulus (G') of the composite films at frequency ranging from 0.1 to 100 Hz. As shown in Figure 5a, G' increases as BN@SPEN increasing, indicating the reinforcement effect of BN@SPEN. In the all range of frequency, G' of PEN and PEN composites show similar changing behavior, suggesting that the BN@SPEN are well dispersed in the PEN matrix. In addition, G' increases obviously at the low frequency when the BN@SPEN loading is higher than 12 wt%, indicating a sudden changing of property in the composites which would be resulted from the formation of percolation network (38). Figure 5b exhibits complex viscosity (η^*) of BN@SPEN/PEN. Firstly, η^* decreases gradually with increasing frequency, indicating the pseudoplastic fluid character of BN@SPEN/PEN. Secondly, η^* increases with increment of BN@SPEN, which demonstrates BN@SPEN/PEN is much more rigid than PEN and acts as reinforce in the system.

3.4 Thermal properties of BN@SPEN/PEN

Figure 6 shows the DSC and TGA results of BN@SPEN/PEN composites. The glass transition temperatures (T_g) of PEN is 208°C. After the incorporation of BN@SPEN, the T_g of the BN@SPEN/PEN composites is almost the same (Table 1), indicating BN@SPEN does not influence the T_g of PEN matrix. In addition, the high T_g suggest high thermal stability of the BN@SPEN/PEN composites

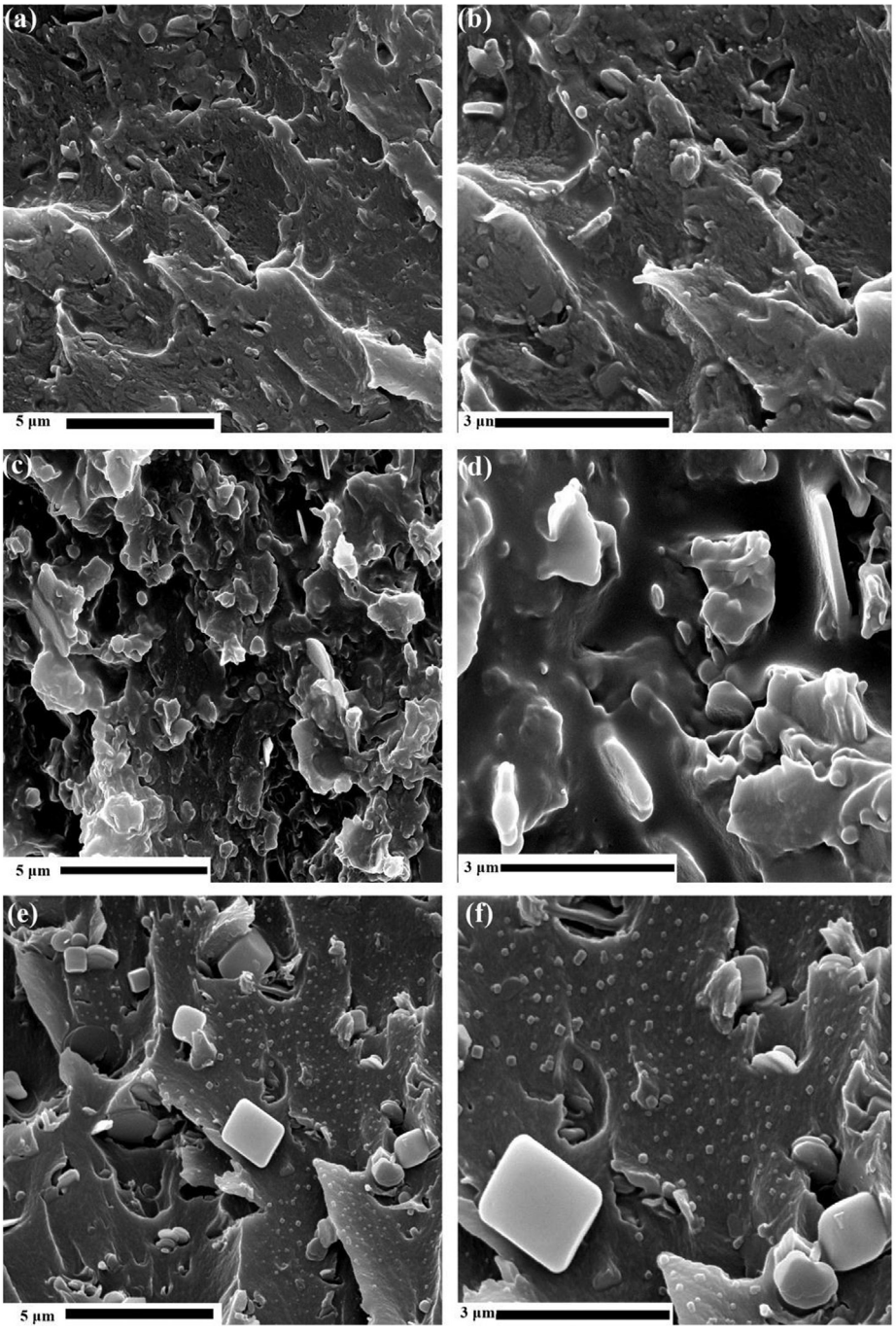

Figure 4: (a) and (b) Cross-sectional SEM images of the BN@SPEN/PEN composite with 8 wt% of BN@SPEN; (c) and (d) SEM images of the BN@SPEN/PEN composite with 20 wt% of BN; (e)-(f) SEM images of the BN/PEN composite film with 8 wt% of BN.

which can be used at high temperature. Figure 6b depicts the TGA curves of the BN@SPEN/PEN composites. The 5 wt% and maximum weight-loss temperature ($T_{5\%}$) and (T_{max}) of PEN used in this study are 517°C and 536°C, respectively (Table 1). The $T_{5\%}$ and T_{max} decrease slightly with the introduction of BN@SPEN. This is due to the lower decomposition temperature of SPEN of BN@SPEN. Nevertheless, the $T_{5\%}$ of the composites is still higher than 470°C, indicating that the composites can be used at high temperature. In addition, the BN content in BN@SPEN/PEN composites is calculated according to the residual mass at 790°C on the TGA curves. The residual mass of PEN, BN@SPEN/PEN4, BN@SPEN/PEN8, BN@SPEN/PEN12,BN@SPEN/PEN16,andBN@SPEN/PEN20

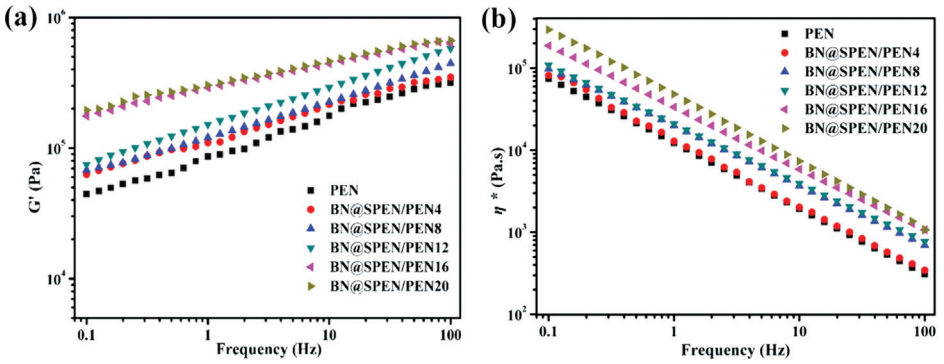

Figure 5: (a) Dynamic storage modulus and (b) complex viscosity of PEN and BN@SPEN/PEN composite films obtained in dynamic frequency sweep from 0.10 to 100 rad/s at 320°C.

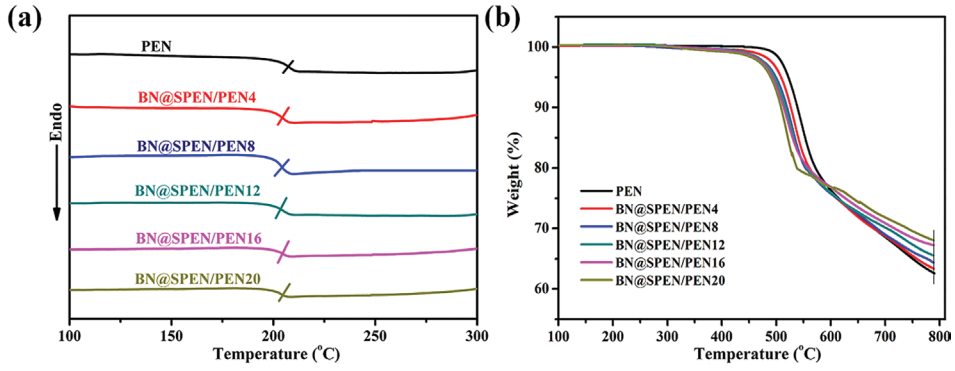

Figure 6: (a) DSC curves of PEN and BN@SPEN/PEN composite films, (b) TGA curves of PEN and BN@SPEN/PEN composite films.

Table 1: Thermal property of PEN and BN@SPEN/PEN composites.

BN@SPEN content	0 wt%	4 wt%	8 wt%	12 wt%	16 wt%	20 wt%
T_g (°C)	208.1	206.0	206.2	206.0	205.2	204.8
$T_{5\%}$ (°C)	517.0	508.2	499.0	489.3	480.0	478.2
T_{max} (°C)	536.1	526.0	519.2	510.3	505.1	502.0

at 790°C is 62.6%, 63.4%, 64.4%, 65.4%, 66.9%, and 67.7% respectively. Therefore, the BN@SPEN content in BN@SPEN/PEN composites is calculated to be 3.3, 7.5, 11.6, 17.8 and 21.1 wt% respectively. Accordingly, the BN content in BN@SPEN/PEN composites is calculated to be 2.4, 5.5, 8.5, 12.9 and 15.4 wt% respectively as the content of BN in BN@SPEN was calculated to be 72.6 wt%.

3.5 Mechanical properties of BN@SPEN/PEN

Mechanical properties of BN@SPEN/PEN composite films with varied mass BN@SPEN are shown in Figure 7. The tensile strength of the BN@SPEN/PEN composite films is presented in Figure 7a. From the illustration, the tensile strength of BN@SPEN/PEN increases as increasing mass fraction of SPEN@BN in the range of 0.0 to 8 wt%. Tensile strength decreases when mass fraction of BN@SPEN/PEN increasing to 12.0 wt%. The tensile modulus of the composite films shows the similar result as that of the tensile strength (Figure 7a, Table 2). Besides, Figure 7b shows the influence of BN@SPEN particles on the breaking elongation of the composite films. It can be seen that elongation at break of the pure film is 10.6% (Table 2). After the incorporation of BN@SPEN particles, there is a trend that the elongation at break decreases with the increasing BN@SPEN mass fraction, which is attributed to the incorporation of BN@SPEN.

3.6 Coefficients of thermal expansion of BN@SPEN/PEN

High coefficient of thermal expansion (CTE) indicates poor dimensional stability and low reliability of the material during its application (39). Therefore, CTE of the materials

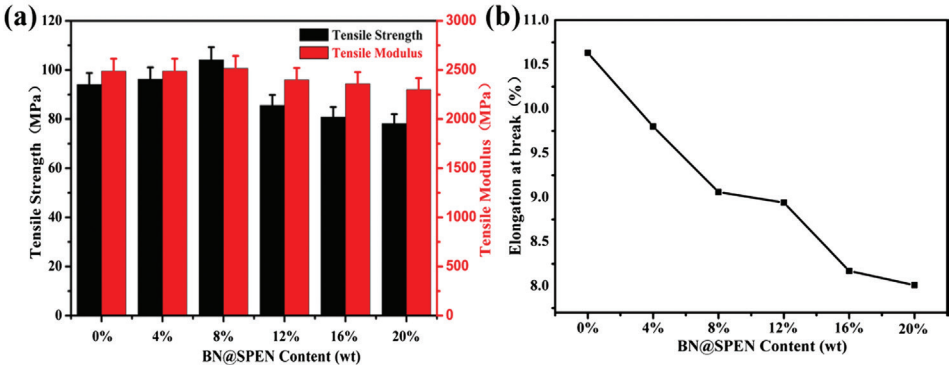

Figure 7: Mechanical properties of PEN and BN@SPEN/PEN composite films: (a) tensile strength and tensile modulus (b) elongation at break.

Table 2: Mechanical properties of PEN and BN@SPEN/PEN composites.

BN@SPEN content	0 wt%	4 wt%	8 wt%	12 wt%	16 wt%	20 wt%
Tensile strength (MPa)	94.1	96.2	104.1	85.6	80.8	78.1
Tensile modulus (MPa)	2489	2433	2517	2400	2360	2301
Elongation at break (%)	10.6	9.8	9.1	8.9	8.2	8.0

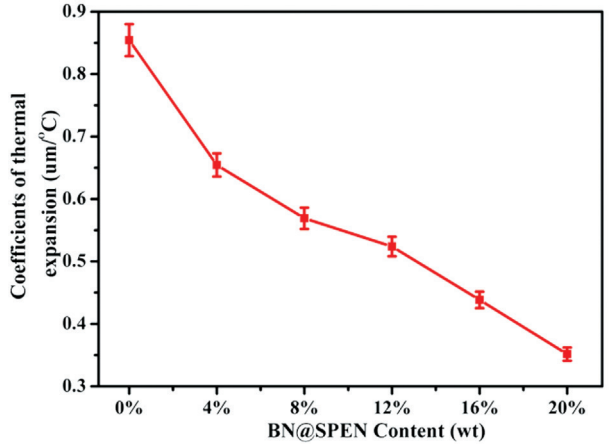

Figure 8: Coefficient of thermal expansion values of BN@SPEN/PEN composite films.

plays a significant role in its application. DMA was employed to investigate CTE of PEN and BN@SPEN/PEN composite. CTE values of the BN@SPEN/PEN composites are shown in Figure 8. The CTE of PEN is as high as 0.85 μm/°C. The CTE decreases to 0.65 μm/°C for BN@SPEN/PEN4 with 4 wt% of BN@SPEN. With the addition of BN@SPEN, the CTE is further reduced, and when used weight of BN@SPEN is 20 wt%, the CTE is as low as 0.35 μm/°C. The well-dispersed BN@SPEN obstruct expansion of PEN chains when temperature arises, which lessen CTE value for the BN@SPEN/PEN composites.

3.7 Thermal conductivity of BN@SPEN/PEN

Figure 9 shows the thermal conductivity of PEN incorporated with different mass fraction of BN@SPEN. Usually, most of the organic polymers are thermal insulators. The thermal conductivity (TC) of PEN is 0.29 W/(m·K), as shown in Figure 9. The results indicate that the addition of BN@SPEN into the polymer matrix increases the thermal conductivity value of PEN composite films obviously. When the BN@SPEN content is 4 wt%, the TC of the BN@SPEN/PEN reaches 0.35 W/(m·K), with an improvement of 21%. When 20 wt% of BN@SPEN is incorporated, the TC of the BN@SPEN/PEN20 is as high as 0.69 W/(m·K), which corresponds to 2.4 fold to that of PEN. In comparing with the composites incorporated with pristine BN (40-42), the thermal conductivity of the

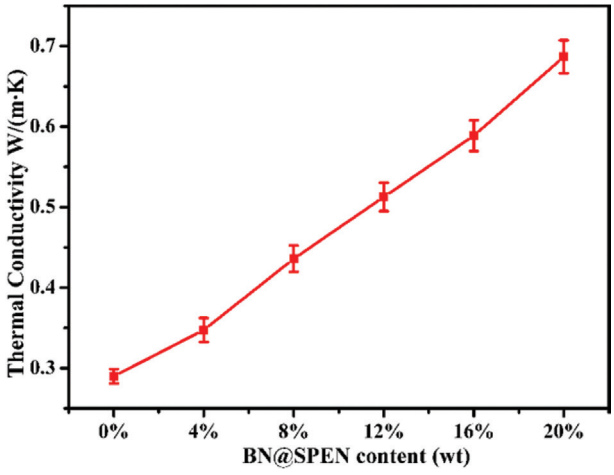

Figure 9: Thermal conductivity of BN@SPEN/PEN composite films.

BN@SPEN/PEN is improved much more obviously at the same content of BN. This is mainly ascribed to the fact that the addition of BN@SPEN effectually minimizes interfacial thermal contact resistance between the PEN and BN. Besides, BN@SPEN serve as conductive channels improving the transportation of thermal phonons of PEN composites.

4 Conclusions

In this article, novel BN@SPEN/PEN composites with PEN as substrate and BN@SPEN as reinforcement were fabricated. BN@SPEN was obtained by ultrasonic method combined with the post-treatment bonding process. The results of FTIR, TGA, SEM and TEM showed the successful coating of BN micro-platelets using the SPEN. The SEM observation and rheology measurement showed that the compatibility between the BN@SPEN and PEN matrix was much better than that between BN and PEN. BN@SPEN/PEN films showed excellent thermal property with T_g exceeding 200°C and $T_{5\%}$ higher than 470°C. Mechanical properties investigation manifested that the BN@SPEN/PEN exhibited superior mechanical properties (tensile strength and Young's modulus higher than 78 MPa and 2300 MPa respectively). Thermal conductivity of BN@SPEN/PEN films was increased to 0.69 W/(m · K) at 20 wt% content of BN@SPEN, showing a 138% increasement comparing with pure PEN.

Acknowledgements: The authors wish to thank for financial supports of this work from the National Natural Science Foundation of China (Project No. 51603029 and 51773028), China Postdoctoral Science Foundation (2017M623001) and National Postdoctoral Program for Innovative Talents (Project No. BX201700044).

References

1. Tong L.F., Wei R.B., Wang J.L., Liu X.B., Phthalonitrile end-capped polyarylene ether nitrile nanocomposites with Cu^{2+} bridged carbon nanotube and graphene oxide network. Mater Lett, 2016, 178, 312-315.
2. Xiao Q., Han W.H., Yang R.Q., You Y., Wei R.B., Liu X.B., Mechanical, dielectric, and thermal properties of polyarylene ether nitrile and boron nitride nanosheets composites. Polym Compos, 2017, 39, E1598-E1605.
3. Wan X.Y., Zhan Y.Q., Zeng G.Y., He Y., Nitrile functionalized halloysite nanotubes/poly (arylene ether nitrile) nanocomposites: interface control, characterization, and improved properties. Appl Surf Sci, 2017, 393, 1-10.
4. Wei R.B., Tu L., You Y., Zhan C.H., Wang Y.J., Liu X.B., Fabrication of crosslinked single-component polyarylene ether nitrile composite with enhanced dielectric properties. Polymer, 2019, 161, 162-169.
5. Wei R.B., Wang J.L., Zhang H.X., Han W.H., Liu X.B., Crosslinked polyarylene ether nitrile interpenetrating with zinc ion bridged graphene sheet and carbon nanotube network. Polymers, 2017, 9, 342.
6. Wei R.B., Li K., Ma J.Y., Zhang H.X., Liu X.B., Improving dielectric properties of polyarylene ether nitrile with conducting polyaniline. J Mater Sci Mater Electron, 2016, 27, 9565-9571.
7. Zhan Y.Q., Wan X.Y., He S.J., Yang Q.B., He Y., Design of durable and efficient poly(arylene ether nitrile)/bioinspired polydopamine coated graphene oxide nanofibrous composite membrane for anionic dyes separation. Chem Eng J, 2018, 333, 132-145.
8. Pu Z.J., Zhou X.F., Yang X.L., Jia K., Liu X.B., One step grafting of iron phthalocyanine containing flexible chains on Fe_3O_4 nanoparticles towards high performance polymer magnetic composites. J Magn Magn Mater, 2015, 385, 368-376.
9. Jin F., Feng M.N., Jia K., Liu X.B., Aminophenoxyphthalonitrile modified MWCNTs/polyarylene ether nitriles composite films with excellent mechanical, thermal, dielectric properties. J Mater Sci Mater Electron, 2015, 26, 5152-5160.
10. Chen Z.R., Lei Y.J., Tang H.L., Wei J.J., Liu X.B., Mechanical, thermal, electrical, and interfacial properties of high-performance bisphthalonitrile/polyarylene ether nitrile/glass fiber composite laminates. Polym Compos, 2013, 34, 2160-2168.
11. Yu C.P., Gong W.B., Tian W., Zhang Q.C., Xu Y.C., Lin Z.Y., et al., Hot-pressing induced alignment of boron nitride in polyurethane for composite films with thermal conductivity over 50 $Wm^{-1} K^{-1}$. Compos Sci Technol, 2018, 160, 199-207.
12. Yang D.J., Wei C., Gong Y.Y., Liu T.X., L V.J., Effects of preparation methods on the mechanical and thermal properties of graphene-modified HNBR composites. e-Polymers, 2018, 18, 57-65.
13. Rao C.N.R., Nag A., Inorganic analogues of graphene. Eur J Inorg Chem, 2010, 27, 4244-4250.
14. Zhang J., Wang X.N., Yu C.P., Li Q.L., Li Z., Li C.W., et al., A facile method to prepare flexible boron nitride/poly(vinyl alcohol) composites with enhanced thermal conductivity. Compos Sci Technol, 2017, 149, 41-47.
15. Duan Z.Q., Liu Y.T., Xie X.M., Ye X.Y., A simple and green route to transparent boron nitride/PVA nanocomposites with significantly improved mechanical and thermal properties. Chinese Chem Lett, 2013, 24, 17-19.
16. Yu C.P., Zhang J., Tian W., Fan X.D., Yao Y.G., Polymer composites based on hexagonal boron nitride and their application in thermally conductive composites. RSC Adv, 2018, 8, 21948-21967.
17. Li T.L., Hsu S.L.C., Enhanced thermal conductivity of polyimide films via a hybrid of micro- and nano-sized boron nitride. J Phys Chem B, 2010, 114, 6825-6829.
18. Shen H., Guo J., Wang H., Zhao N., Xu J., Bioinspired Modification of h-BN for High Thermal Conductive Composite Films with Aligned Structure. ACS Appl Mater Interfaces, 2015, 7, 5701-5708.
19. May P., Khan U., Hughes J.M., Coleman J.N., Role of solubility parameters in understanding the steric stabilization of exfoliated two-dimensional nanosheets by adsorbed polymers. J Phys Chem C, 2012, 116, 24390-24391.

20. Coleman J.N., Lotya M., O'Neill A., Bergin S.D., King P.J., Khan U., et al., Two-dimensional nanosheets produced by liquid exfoliation of layered materials. Science, 2011, 331, 568-571.
21. Lee K.H., Shin H.J., Lee J., Lee I.Y., Kim G.H., Choi J.Y., et al., Large-scale synthesis of high-quality hexagonal boron nitride banosheets for large-area graphene electronics. Nano Lett, 2012, 12, 714-718.
22. Yu C.P., Gong W.B., Zhang J., Lv W.B., Tian W., Fan X.D., et al., Hot pressing-induced alignment of hexagonal boron nitride in SEBS elastomer for superior thermally conductive composites. RSC Adv, 2018, 8, 25835-25845.
23. Yu C.P., Zhang J., Li Z., Tian W., Wang L.J., Luo J., et al., Enhanced through-plane thermal conductivity of boron nitride/epoxy composites. Composites, Part A, 2017, 98, 25-31.
24. Safikhani M.M., Zamanian A., Ghorbani F., Synergistic effects of retinoic acid and graphene oxide on the physicochemical and in-vitro properties of electrospun polyurethane scaffolds for bone tissue engineering. e-Polymers, 2017, 17, 363-371.
25. Lei W., Mochalin V.N., Liu D., Qin S., Gogotsi Y., Chen Y., Boron nitride colloidal solutions, ultralight aerogels and freestanding membranes through one-step exfoliation and functionalization. Nat Commun, 2015, 6, 8849-8856.
26. Wang X.B., Zhi C.Y., Li L., Zeng H.B., Li C., Mitome M., et al., "Chemical blowing" of thin-walled bubbles: high-throughput fabrication of large-area, few-layered BN and C_x-BN nanosheets. Adv Mater, 2011, 23, 4072-4076.
27. Zhi C., Bando Y., Tang C.C., Kuwahara H., Golberg D., Large-scale fabrication of boron nitride nanosheets and their utilization in polymeric composites with improved thermal and mechanical properties. Adv Mater, 2009, 21, 2889-2895.
28. Tong L.F., Jia K., Liu X.B., Novel phthalonitrile-terminated polyarylene ether nitrile with high glass transition temperature and enhanced thermal stability. Mater Lett, 2014, 128, 267-270.
29. Feng M.N., Meng F.B., Pu Z.J., Jia K., Liu X.B., Introducing magnetic-responsive CNT/Fe3O4 composites to enhance the mechanical properties of sulfonated poly(arylene ether nitrile) proton-exchange membranes. J Polym Res, 2015, 3, 22-27.
30. Lee D.J., Lee B., Park K.H., Ryu H.J., Jeon S., Hong S.H., Scalable exfoliation process for highly soluble boron nitride nanoplatelets by hydroxide-assisted ball milling. Nano Lett. 2015, 15, 1238-1244.
31. Yuan F., Jiao W.C., Yang F., Liu W.B., Liu J.Y., Xu Z.H., et al., Scalable exfoliation for large-size boron nitride nanosheets by low temperature thermal expansion-assisted ultrasonic exfoliation. J Mater Chem C, 2017, 5, 6359-6368.
32. Wu X., Liu H., Tang Z.H., Guo B.C., Scalable fabrication of thermally conductive elastomer/boron nitride nanosheets composites by slurry compounding. Compos Sci Technol, 2016, 123, 179-186.
33. Lin Y., Williams T.V., Xu T.B., Cao W., Elsayed-Ali H.E., Connell J.W., Aqueous dispersions of few-layered and monolayered hexagonal boron nitride nanosheets from sonication-assisted hydrolysis: critical role of water. J Phys Chem C, 2011, 115, 2679-2685.
34. Wang Y., Shi Z.X., Yin J., Boron nitride nanosheets: large-scale exfoliation in methanesulfonic acid and their composites with polybenzimidazole. J Mater Chem, 2011, 21, 11371-11377.
35. Sainsbury T., Satti A., May P., O'Neill A., Nicolosi V., Gun'ko Y.K., et al., Covalently functionalized hexagonal boron nitride nanosheets by nitrene addition. Chem Eur J, 2012, 18, 10808-10812.
36. Feng M.N., Jin F. Huang X., Jia K., Liu X.B., In situ fabrication of MWCNTs reinforce dielectric performances of polyarylene ether nitrile nanocomposite. J Mater Sci: Mater Electron, 2015, 26, 1-10.
37. Feng M.N., Huang X., Tang H.L., Liu X.B., Effects of surface modification on interfacial and rheological properties of CCTO/PEN composite films. Colloids Surf A, 2014, 441, 556-564.
38. Qian J., Fu C., Wu X.Y., Ran X.H., Nie W., Promotion of poly(vinylidene fluoride) on thermal stability and rheological property of ethylene-tetrafluoroethylene copolymer. e-Polymers, 2018, 18, 541-549.
39. Zhang D.S., Li K.Z., Li H.J., Jia Y., Guo L., Li H.L., Coefficients of thermal expansion of low texture and isotropic pyrocarbon deposited on stationary substrates. Mater Lett, 2012, 68, 68-70.
40. Lei Y.X., Han Z.M., Ren D.X., Pan H., Xu M.Z., Liu X.B., Design of h-BN-filled cyanate/epoxy thermal conductive composite with stable dielectric properties. Macromol Res, 2018, 1-7.
41. Yang N., Xu C., Hou J., Yao Y.M., Zhang Q.X., Qu X.W., Preparation and properties of thermally conductive polyimide/boron nitride composites. RSC Adv, 2016, 6, 18279-18287.
42. Cheewawuttipong W., Fuoka D., Tanoue S., Uematsu H., Iemoto Y., Thermal and mechanical properties of polypropylene/boron nitride composites. Energy Procedia, 2013, 34, 808-817.